International Journal of Thermal Sciences 49 (2010) 1–9

Contents lists available at ScienceDirect

International Journal of Thermal Sciences

journal homepage: www.elsevier.com/locate/ijts

Periodic natural convection in a nanofluid-filled enclosure with oscillating heat flux

B. Ghasemi [a,*], S.M. Aminossadati [b,1]

[a] Shahrekord University, Faculty of Engineering, PO Box 115, Shahrekord, Iran
[b] The University of Queensland, School of Mechanical and Mining Engineering, QLD 4072, Australia

ARTICLE INFO

Article history:
Received 4 March 2009
Received in revised form
22 July 2009
Accepted 22 July 2009
Available online 14 August 2009

Keywords:
Periodic natural convection
Enclosure
Nanofluids
Oscillating heat flux

ABSTRACT

This paper examines the periodic natural convection in an enclosure filled with nanofluids. Whilst a heat source with oscillating heat flux is located on the left wall of the enclosure, the right wall is maintained at a relatively low temperature and the other walls are thermally insulated. Based upon numerical predictions, the effects of pertinent parameters such as Rayleigh number, solid volume fraction, heat source position, type of nanoparticles and oscillation period are examined. A periodic behaviour is found for the flow and temperature fields as a result of the oscillating heat flux. The utilisation of nanoparticles, in particular Cu, enhances the heat transfer especially at low Rayleigh numbers. In addition, the oscillation period of heat generation affects the maximum operational temperature of the heat source. It is also interesting to observe that the optimum position of the heat source on the left wall is a function of Rayleigh number. The results of this study can be used in the design of an effective cooling system for electronic components to help ensure effective and safe operational conditions.

1. Introduction

Due to its various applications, buoyancy-driven heat transfer in enclosures filled with clear fluids has been comprehensively studied and documented in the literature in the past [1]. In particular, attention has been given to enclosures with time-dependent thermal boundary conditions due to their relevance in practical situations such as heating or cooling of buildings, food storage facilities and heat removal from electronic components.

For the first time, Lage and Bejan [2] investigated the buoyancy-driven flows in a square enclosure with periodic heat flux and examined the effects of oscillation frequency of heat generation on natural convection. Other researchers carried out similar studies by considering a clear base fluid within the enclosure [3–6]. For an air-filled enclosure, Xia et al. [7] studied the stability of buoyancy-driven laminar flows where sinusoidal perturbation was imposed on the hot vertical wall. They argued that the perturbation destabilises the flow in high amplitudes leading to lower critical Rayleigh numbers for the flow transitions. For a water-filled enclosure, Antohe and Lage [8] experimentally examined the pulsating horizontal heating process and showed that by tuning the heating oscillation period properly, the heat transfer across the enclosure can be enhanced.

Most of the studies on natural convection under oscillating thermal boundary conditions have utilised the base fluid with a low thermal conductivity, which, in turn, limits the heat transfer enhancement. Choi [9] showed that introducing nanofluids containing nanoparticles with substantially higher thermal conductivities improves the heat transfer performance. The results of this study have also been confirmed by other researchers [10–13].

However, contradictory studies can be found which argue that the dispersion of nanoparticles in the base fluid may result in considerable decrease in the heat transfer [14–16]. Ho et al. [17] argued that the enhancement or mitigation of heat transfer depends on the formulas used for the thermal properties for nanofluids. Even though the structure, shape, size, aggregation and anisotropy of the nanoparticles as well as the type, fabrication process, particle aggregation and deterioration of nanofluids are important factors in a comprehensive nanofluid modelling study, many researchers still find the classical models to be appropriate for predicting the physical properties of nanofluids [18–20].

The utilisation of nanofluids for cooling enhancement of systems with an oscillating heat flux can be considered as an area of interest for the designers of heat removal systems in the electronic industry. To the best knowledge of the authors, no study has yet been reported on this topic in the literature. As such, the focus of

* Corresponding author. Tel./fax: +98 381 4424438.
E-mail addresses: behzadgh@yahoo.com, ghasemi@eng.sku.ac.ir (B. Ghasemi), uqsamino@uq.edu.au (S.M. Aminossadati).
[1] Tel.: +61 7 33653676; fax: +61 7 33653888.

1290-0729/$ – see front matter © 2009 Elsevier Masson SAS. All rights reserved.
doi:10.1016/j.ijthermalsci.2009.07.020

Nomenclature

C_p	specific heat, J/kg K
g	gravitational acceleration, m/s^2
h	convection heat transfer coefficient, W/m^{2}K
h_s	heat source length, m
H_s	dimensionless heat source length (h_s/L)
k	thermal conductivity, W/mK
L	enclosure length, m
Nu_s	local Nusselt number on the heat source
Nu_m	average Nusselt number
p	fluid pressure, Pa
$\overline{p}$	modified pressure ($p+\rho_c g y$)
P	dimensionless pressure ($\overline{p}L^2/\rho_{nf}\alpha_f^2$)
Pr	Prandtl number (ν_f/α_f)
q''	oscillating heat flux, W/m^2
q''_0	amplitude of oscillating heat flux, W/m^2
Ra	Rayleigh number ($g\beta_f L^3\Delta T/\nu_f\alpha_f$)
S_φ	source term in Eq. (2)
t	time, s
t_p	oscillation period, s
T	temperature, K
u,v	velocity components in x,y directions, m/s
U,V	dimensionless velocity components (uL/α_f, vL/α_f)
x,y	cartesian coordinates, m
X,Y	dimensionless coordinates (x/L, y/L)
y_s	distance of the heat source from the bottom wall, m
Y_s	dimensionless distance of the heat source from the bottom wall (y_s/L)

Greek symbols

α	thermal diffusivity, m^2/s
β	thermal expansion coefficient, 1/K
ΔT	temperature difference $\Delta T = q''_0 L/k_f$
ϕ	solid volume fraction
φ	non-dimensional parameter in Eq. (2)
Γ_φ	diffusion term in Eq. (2)
μ	Dynamic viscosity, Ns/m^2
ν	kinematic viscosity, m^2/s
θ	dimensionless temperature $(T-T_c)/\Delta T$
θ_{max}	maximum heat source temperature along its length
$(\theta_{max})_{max}$	the highest value of θ_{max} respect to time
$(\theta_{max})_{min}$	the lowest value of θ_{max} respect to time
ρ	density, kg/m^3
τ	time in dimensionless form ($\alpha_f t/L^2$)
τ_p	oscillation period in dimensionless form ($\alpha_f t_p/L^2$)
ψ_{max}	maximum stream function

Subscripts

c	cold wall
f	fluid (pure water)
nf	nanofluid
np	nanoparticle
s	heat source

the present study is to examine the effects of pertinent parameters such as Rayleigh number, solid volume fraction, heat source position, type of nanoparticles and oscillation period on the natural convection cooling characteristics of an enclosure with an oscillating heat flux.

2. Problem description

Fig. 1 depicts the geometry of the square enclosure filled with nanofluids. The right wall of the enclosure is maintained at a uniform low temperature (T_c) while the other walls are thermally insulated. A partial heat source with an oscillating heat flux (Eq. (1)) is embedded on the left vertical wall of the enclosure. The oscillating heat flux simulates the heat generation by an electronic component having a pulsating input voltage [21].

$$q'' = q''_0\left[1+\cos\left(\frac{2\pi t}{t_p}\right)\right]. \quad (1)$$

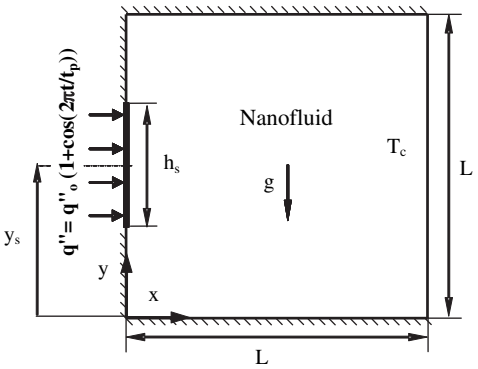

Fig. 1. A schematic diagram of the physical model.

The enclosure is filled with a water-based nanofluid ($Pr = 6.2$) containing various spherical nanoparticles (Cu, Al_2O_3 and TiO_2). It is assumed that the base fluid and the nanoparticles are in thermal equilibrium, the nanofluid is Newtonian and incompressible and the flow is laminar. The thermophysical properties of the base fluid and the nanoparticles are given in Table 1. Constant thermophysical properties are considered for the nanofluid except for the density variation in the buoyancy forces determined by using the Boussinesq approximation.

3. Governing equations

The equations that govern the conservation of mass, momentum and energy can be written in a non-dimensional form as shown in Eq. (2).

Table 1
Thermophysical properties of pure water and nanoparticles.

Physical properties	Pure water	Cu	Al_2O_3	TiO_2
ρ (kg/m^3)	997.1	8933	3970	4250
C_P (J/kg K)	4179	385	765	686.2
k (W/mK)	0.613	400	40	8.9538
β (1/K)	21×10^{-5}	1.67×10^{-5}	0.85×10^{-5}	0.9×10^{-5}

Table 2
A summary of the governing non-dimensional equations.

Equations	φ	Γ_φ	S_φ
Continuity	1	0	0
X-momentum	U	$\mu_{nf}/\rho_{nf}\alpha_f$	$-(\partial P/\partial X)$
Y-momentum	V	$\mu_{nf}/\rho_{nf}\alpha_f$	$-(\partial P/\partial Y)+((\rho\beta)_{nf}/\rho_{nf}\beta_f)\,Ra\,Pr\,\theta$
Energy	θ	α_{nf}/α_f	0

Table 3
Applied models for the formulation of the nanofluids properties.

Nanofluid properties	Applied model
Density	$\rho_{nf}=(1-\phi)\rho_f+\phi\rho_{np}$
Thermal diffusivity	$\alpha_{nf}=k_{nf}/(\rho C_p)_{nf}$
Heat capacitance	$(\rho C_p)_{nf}=(1-\phi)(\rho C_p)_f+\phi(\rho C_p)_{np}$
Thermal expansion coefficient	$(\rho\beta)_{nf}=(1-\phi)(\rho\beta)_f+\phi(\rho\beta)_{np}$
Dynamic viscosity [23]	$\mu_{nf}=\mu_f/(1-\phi)^{2.5}$
Thermal conductivity [18–20,24]	$k_{nf}=k_f[(k_{np}+2k_f)-2\phi(k_f-k_{np})/(k_{np}+2k_f)+\phi(k_f-k_{np})]$

$$\frac{\partial\varphi}{\partial\tau}+\frac{\partial(U\varphi)}{\partial X}+\frac{\partial(V\varphi)}{\partial Y}=\frac{\partial}{\partial X}\left(\Gamma_\varphi\frac{\partial\varphi}{\partial X}\right)+\frac{\partial}{\partial Y}\left(\Gamma_\varphi\frac{\partial\varphi}{\partial Y}\right)+S_\varphi. \quad (2)$$

where, φ stands for the dependent non-dimensional parameters U, V and θ, and Γ_φ and S_φ are the corresponding diffusion and source terms, respectively, as summarised in Table 2. The properties of the nanofluids are determined based on the models presented in Table 3. The non-dimensional groups presented in Eq. (3) are used in the present analysis.

$$X=\frac{x}{L},\ Y=\frac{y}{L},\ \tau=\frac{\alpha_f t}{L^2},\ U=\frac{uL}{\alpha_f},\ V=\frac{vL}{\alpha_f},\ P=\frac{\overline{p}L^2}{\rho_{nf}\alpha_f^2},$$
$$\theta=\frac{T-T_c}{\Delta T},\ Ra=\frac{g\beta_f L^3(\Delta T)}{\nu_f\alpha_f},\ \Delta T=\frac{q_0'' L}{k_f},\ Pr=\frac{\nu_f}{\alpha_f} \quad (3)$$

The non-dimensional initial conditions are $U=V=0$ and $\theta=0$ and the non-dimensional boundary conditions are as follows:

Table 4
Comparison between the present work and other studies for Nu_m (air-filled enclosure).

	$Ra=10^3$	$Ra=10^4$	$Ra=10^5$	$Ra=10^6$
De Vahl Davis [25]	1.118	2.243	4.519	8.799
Markatos and Pericleous [26]	1.108	2.201	4.430	8.754
Hadjisophocleous et al. [27]	1.141	2.290	4.964	10.390
Tiwari and Das [28]	1.087	2.195	4.450	8.803
Present work	1.118	2.248	4.547	8.980
Difference with De Vahl Davis [25] (%)	0.00	0.22	0.62	2.06

$$\begin{aligned}&1.\text{On the walls of the enclosure}: U=V=0\\&2.\text{On the right wall}: \theta=0\\&3.\text{On the insulated walls}: \frac{\partial\theta}{\partial X}=0,\ \text{or}\ \frac{\partial\theta}{\partial Y}=0\\&4.\text{On the heat source}: \left(\frac{\partial\theta}{\partial X}\right)_{X=0}=-\left(\frac{k_f}{k_{nf}}\right)\left[1+\cos\left(\frac{2\pi\tau}{\tau_p}\right)\right]\end{aligned} \quad (4)$$

where, $\tau_p=\alpha_f t_p/L^2$ is the non-dimensional form of the heat flux oscillation period.

4. Numerical approach

The control volume formulation given by Patankar [22] and the SIMPLE algorithm are utilised to solve the governing Eq. (2) with the corresponding boundary conditions given in Eq. (4). The convection–diffusion terms are discritized by a power-law scheme and the system is numerically modelled in FORTRAN. After solving the governing equations for U, V and θ, other useful quantities such

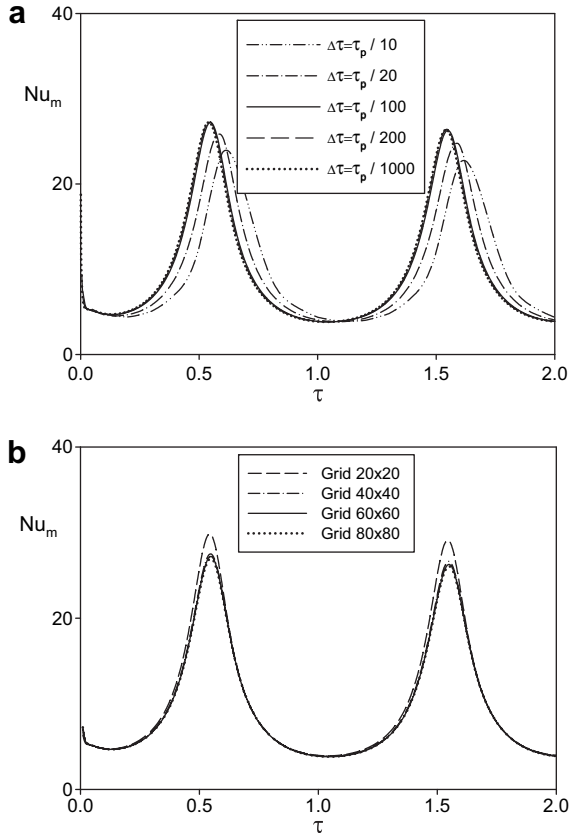

Fig. 2. a: Time step independency study: Nu_m at different time steps. b. Grid independency study: Nu_m at different grid densities.

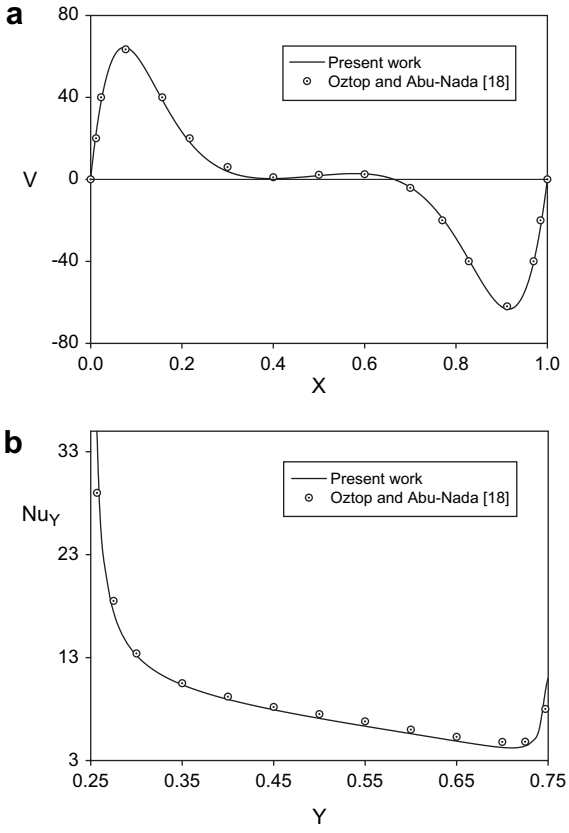

Fig. 3. a: Code validation for a water-Cu nanofluid against Oztop and Abu-Nada [18]: Fig. 11. b: Code validation for a water-Cu nanofluid against Oztop and Abu-Nada [18]: Fig. 12.

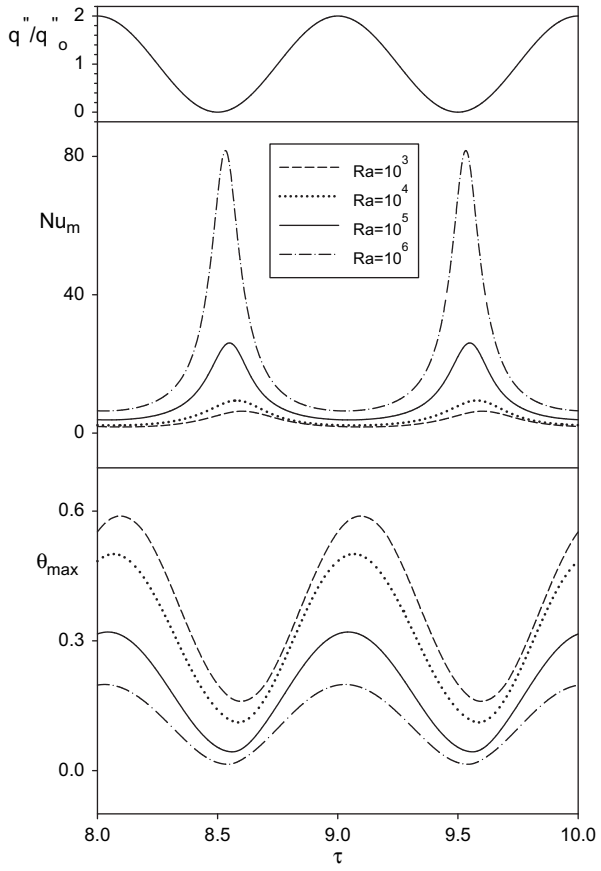

Fig. 4. Periodic-state time history of Nu_m and θ_{max} for various Ra (water-Cu nanofluid, $\varphi = 0.1$, $Y_s = 0.5$, $\tau_p = 1$).

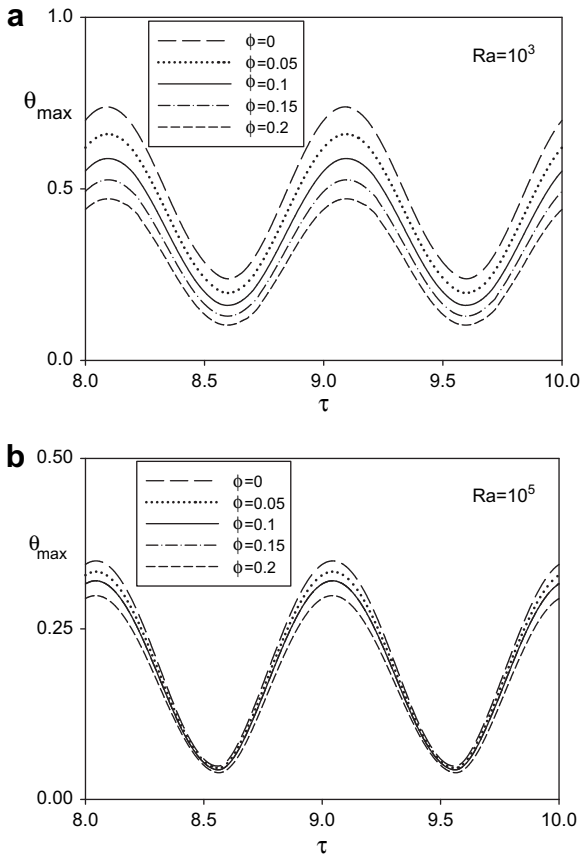

Fig. 5. a: Periodic-state time history of θ_{max} for different ϕ (water-Cu nanofluid, $Y_s = 0.5$, $\tau_p = 1$, $Ra = 10^3$). b: Periodic-state periodic time history of θ_{max} for different ϕ (water-Cu nanofluid, $Y_s = 0.5$, $\tau_p = 1$, $Ra = 10^5$).

as Nusselt number can be determined. The local Nusselt number on the heat source surface can be defined as

$$Nu_s = \frac{hL}{k_f}. \tag{5}$$

where, h is the convection heat transfer coefficient and can be considered as

$$h = \frac{q''_0}{T_s - T_c}. \tag{6}$$

Rearranging the local Nusselt number by using the dimensionless parameters in Eq. (3) yields:

$$Nu_s(Y) = \frac{1}{\theta_s(Y)}. \tag{7}$$

The average Nusselt number is determined by integrating Nu_s along the heat source.

$$Nu_m = \frac{1}{H_s} \int_{Y_s - 0.5H_s}^{Y_s + 0.5H_s} Nu_s(Y)\mathrm{d}Y. \tag{8}$$

5. Time step and grid independency studies

The time step independency study is carried out for a mesh size of 60×60 and five different time steps. The enclosure is filled with a water-Cu nanofluid ($\phi = 0.1$, $Ra = 10^5$, $\tau_p = 1$, $Y_s = 0.5$ and $H_s = 0.4$). According to the results for the periodic-state time history of Nu_m (Fig. 2a), an optimal time step of $\Delta\tau = \tau_p/100$ is adopted for all the subsequent computations. This is also checked by considering other values of oscillation period ($\tau_p = 0.01$ and 100) and the same result is obtained. The grid independency study is also carried out by considering a time step of $\Delta\tau = \tau_p/100$ and four different mesh sizes. For each mesh size and for the same conditions mentioned earlier, the periodic-state time history of Nu_m is plotted in Fig. 2b. It is found that a grid size of 60×60 is adequate to ensure the grid

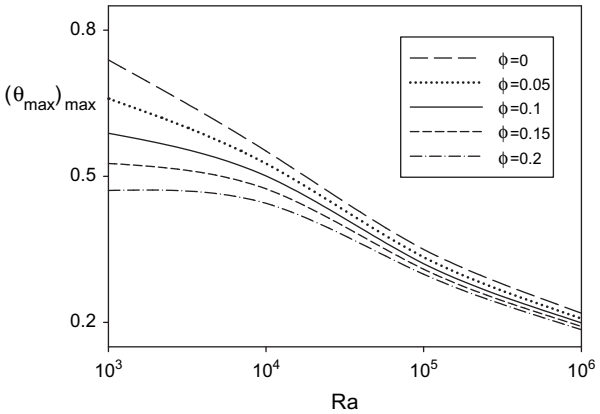

Fig. 6. The effects of Ra on $(\theta_{max})_{max}$ for different ϕ (water-Cu nanofluid, $Y_s = 0.5$, $\tau_p = 1$).

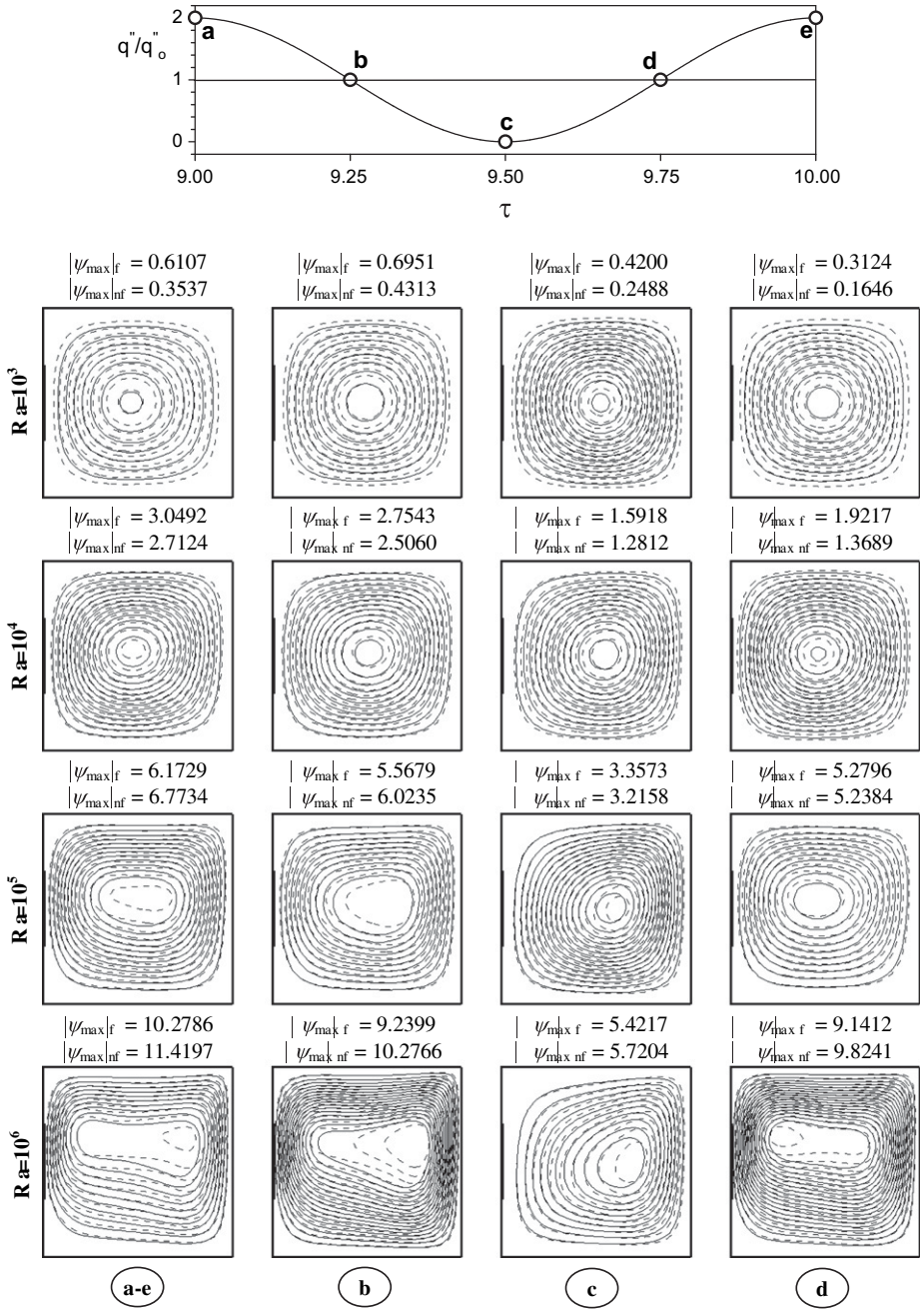

Fig. 7. Flow patterns at different *Ra* and time stages for a water-Cu nanofluid, $\phi = 0.1$(—) and pure water (- - -).

independency. The convergence criteria is to reduce the maximum mass residual of the grid control volume below 10^{-7}.

6. Code validation

In order to validate the present code, the average Nusselt number, Nu_m, calculated for natural convection in a differentially heated enclosure filled with air is compared against the values reported by other researchers (Table 4). It is found that the present results compare very well with other reported values. In addition, the present code is further validated against the work by Oztop and Abu-Nada [18] in terms of *Y*-velocity at the mid section of the enclosure, *V* (Fig. 3a) and local Nusselt number along the left wall, Nu_Y (Fig. 3b). In this study, an enclosure filled with a water-Cu nanofluid ($\phi = 0.1$, $Ra = 105$, $Y_s = 0.5$ and $H_s = 0.4$) is considered. It is clear that the results for *V* and Nu_Y are in good agreement with the results reported in the literature.

7. Results

7.1. Rayleigh number and solid volume fraction

For this part of the analysis, an enclosure filled with a water-Cu nanofluid is considered. An oscillating heat source with a length of $H_s = 0.4$ and an oscillation period of $\tau_p = 1$ is modelled in the middle of the left vertical wall ($Y_s = 0.5$).

Fig. 4 shows the periodic-state time history of the average Nusselt number (Nu_m) and the maximum temperature (θ_{max}) of the

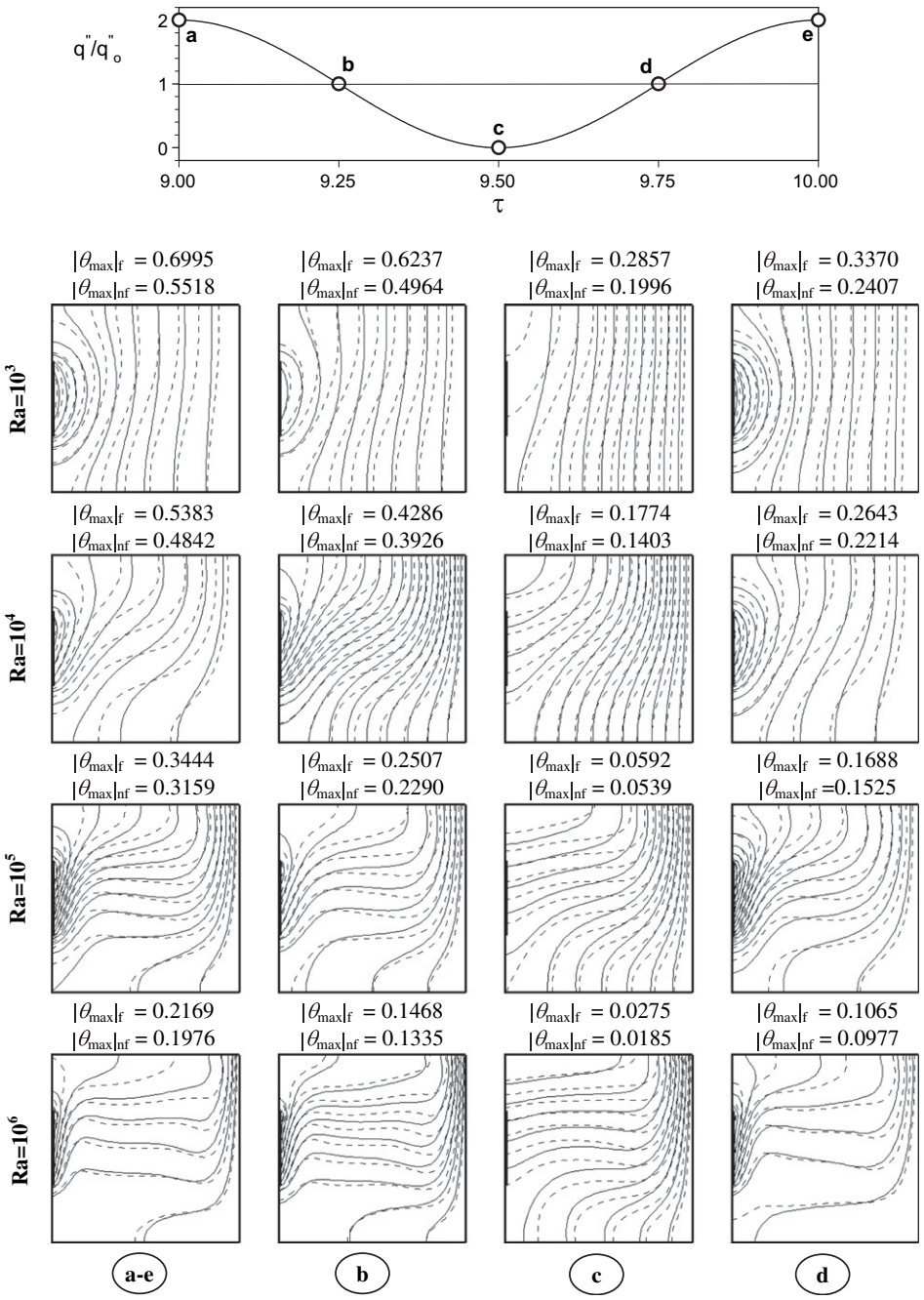

Fig. 8. Isotherms at different *Ra* and time stages for a water-Cu nanofluid, $\phi = 0.1$ (—) and pure water (–).

heat source for two complete oscillation periods after they reach a periodic-state situation. In order to examine how Nu_m and θ_{max} follow the oscillations of the heat flux, the periodic variation of the heat flux ratio (q''/q''_0) is also plotted at the top of this figure. It is evident that the oscillations of Nu_m and θ_{max} have a similar response frequency but with a slight phase shift. It is also found that as Rayleigh number increases due to strengthening buoyancy-driven flows, the rate of heat transfer from the heat source increases. This, in turn, lowers the heat source maximum temperature which plays an important role in the design of electronic components.

One of the objectives of this research is to investigate the influence of nanofluids on the cooling performance of electronic components with periodic heat generation. Thus, it is a subject of interest to examine how the solid volume fraction of nanoparticles affects the cooling enhancement. Fig. 5 shows that for both $Ra = 10^3$ and 10^5, the addition of Cu nanoparticles into pure water lowers the heat source maximum temperature. It can also be seen that the maximum temperature decreases with an increase in the solid volume fraction of nanoparticles; however, this increase is more pronounced at low Rayleigh numbers, where conduction dominates the heat transfer mechanism and the addition of nanoparticles with relatively higher thermal conductivity improves the conduction heat transfer rate.

The variation of the highest value of the heat source maximum temperature, $(\theta_{max})_{max}$, with respect to time is examined in Fig. 6. In fact, the values of $(\theta_{max})_{max}$ correspond to the θ_{max} oscillation peaks presented in Fig. 5. It must be noted that $(\theta_{max})_{max}$ is a crucial

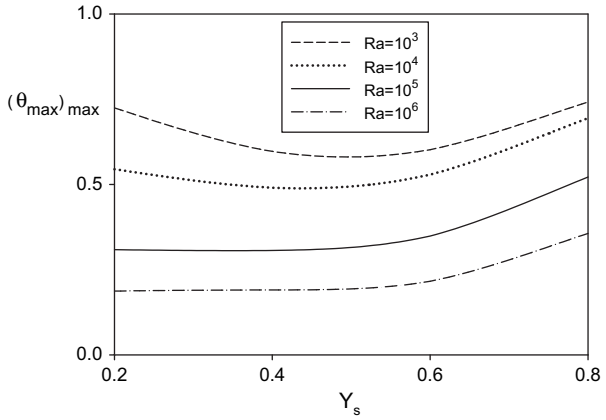

Fig. 9. The effects of heat source location on $(\theta_{max})_{max}$ at different *Ra* (water-Cu nanofluid, $\phi = 0.1$, $\tau_p = 1$).

design parameter for electronic components. The greater the reduction of $(\theta_{max})_{max}$, the safer and longer the electronic components operate. The results show that $(\theta_{max})_{max}$ can be lowered by increasing Rayleigh number or by adding nanoparticles into the pure water. For an enclosure filled with a water-Cu nanofluid ($Y_s = 0.5$, $H_s = 0.4$ and $\tau_p = 1$), a general correlation is obtained for predicting $(\theta_{max})_{max}$ as a function of Rayleigh number and solid volume fraction.

$$(\theta_{max})_{max} = \frac{0.4705 - \phi}{0.9167 + 2.44 \times 10^{-5} Ra} + 0.1952. \quad (9)$$

Figs. 7 and 8 show the streamlines and isotherms, respectively, for both pure water (- - -) and the water-Cu nanofluid (—). The results are presented for four different Rayleigh numbers ($10^3 \le Ra \le 10^6$) and five different stages of a complete periodic-state cycle of heat generation as presented at the top of the figures. [$(a)\tau = 9$ $(b)\tau = 9 + \tau_p/4$ $(c)\tau = 9 + \tau_p/2$ $(d)\tau = 9 + 3\tau_p/4$ $(e)\tau = 9 + \tau_p$]. It is clear that at $Ra = 10^3$, for both the nanofluid and pure water, the clockwise circulation cells are relatively weak and the isotherms are rather vertical within the enclosure indicating conduction heat transfer. Moreover, the isotherms for the nanofluid tend to be more vertical indicating stronger conduction heat transfer for the nanofluid compared to pure water. It is also clear that an increase of Rayleigh number is associated with higher values of stream function and lower values of maximum temperature as a result of strengthening the buoyancy-induced flow field. It is interesting to see that the minimum value of the stream function is achieved at stage $(c)\tau = 9 + \tau_p/2$, where the magnitude of heat flux goes to zero, however, at this stage the lowest maximum temperature is also obtained because there is no heat generation source in the enclosure.

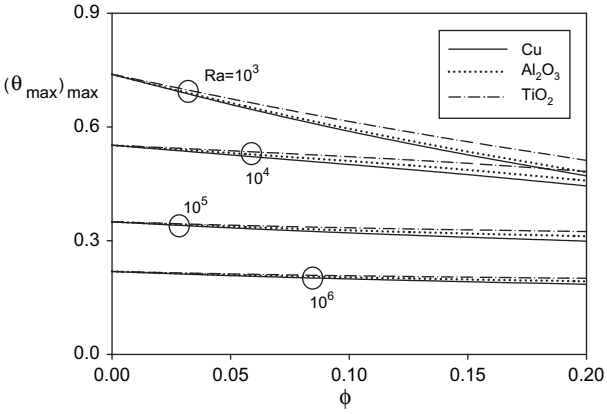

Fig. 10. The effects of different nanoparticles volume fractions on $(\theta_{max})_{max}$ at different *Ra* ($Y_s = 0.5$, $\tau_p = 1$).

7.2. Heat source position

This section examines how the position of the heat source on the left wall affects the cooling performance of the enclosure. The enclosure is filled with a water-Cu nanofluid ($\phi = 0.1$, $H_s = 0.4$ and $\tau_p = 1$). The variation of $(\theta_{max})_{max}$ in Fig. 9 shows that at $Ra = 10^3$, where heat transfer is mainly due to conduction, a better cooling enhancement is achieved when the heat source is in the middle of the left wall ($Y_s = 0.5$). However, at higher Rayleigh numbers, better cooling is associated with lower positions of the heat source on the left wall. This is because at low positions, the heat source is in contact with a stronger buoyancy-induced circulating flow with a relatively lower temperature removing more heat from the heat source and lowering its temperature. As the heat source moves upwards, the power of circulating flow decreases and as a result, its temperature increases by the time it reaches the heat source. Thus, less heat is removed from the heat source resulting in higher temperatures.

7.3. Type of nanofluid

The influence of different types of nanofluids on $(\theta_{max})_{max}$ is examined in Fig. 10 using three different nanoparticles (Cu, Al_2O_3

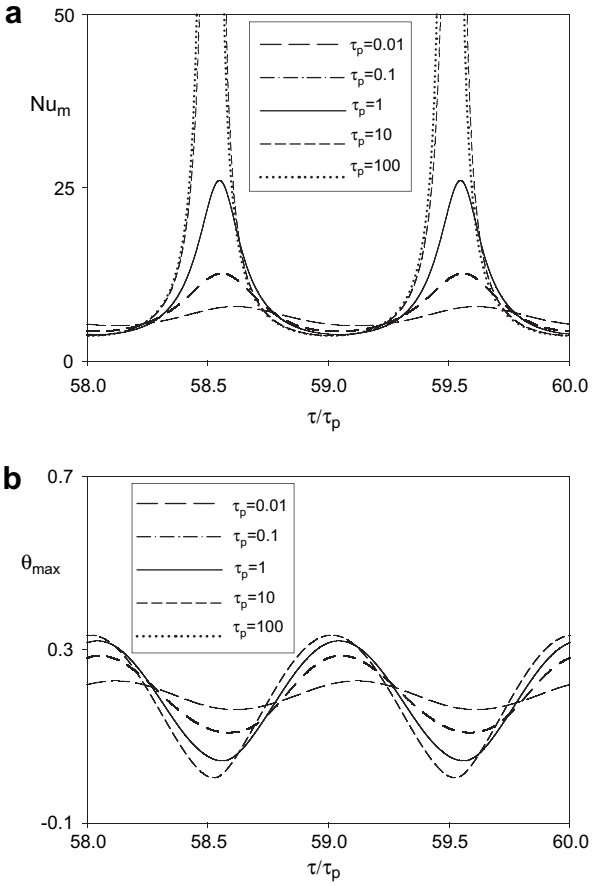

Fig. 11. . a: Periodic-state time history of Nu_m at various oscillation periods (water-Cu nanofluid, $\phi = 0.1$, $Y_s = 0.5$, $Ra = 10^5$). b: Periodic-state time history of θ_{max} at various oscillation periods (water-Cu nanofluid, $\phi = 0.1$, $Y_s = 0.5$, $Ra = 10^5$).

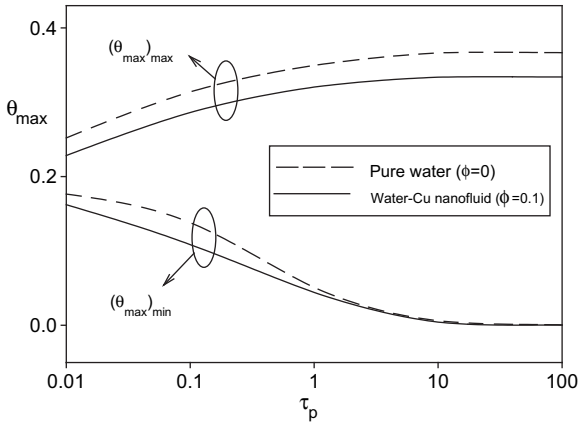

Fig. 12. A comparison between pure water and a water-Cu nanofluid ($\phi = 0.1$) for the variation of $(\theta_{max})_{max}$ and $(\theta_{max})_{min}$ with the oscillation period ($Y_s = 0.5$, $Ra = 10^5$).

and TiO_2) and various solid volume fractions ($0 \le \phi \le 0.2$). The heat source with a length of $H_s = 0.4$ is considered in the middle of the left wall ($Y_S = 0.5$). For all Rayleigh numbers, the highest values of $(\theta_{max})_{max}$ correspond to the nanofluid having TiO_2 nanoparticles which have the lowest value of thermal conductivity compared to other nanoparticles (Table 1). On the other hand, Cu nanoparticles with the highest thermal conductivity encompass the maximal heat removal effectiveness resulting in the lowest temperature for the heat source.

7.4. Oscillation period

The heat generation oscillation period plays a critical role in the cooling mechanism of electronic components [8]. It is interesting to know how the maximum temperature of the heat source varies with the oscillation period. Fig. 11 shows the periodic-state oscillation of Nu_m and θ_{max} for two complete periodic cycles at different oscillation periods. For a better comparison of the periodic results, dimensionless time on the horizontal axis is normalised by τ_p. In this study, the enclosure is filled with a water-Cu nanofluid ($\phi = 0.1$, $H_s = 0.4$, $Y_s = 0.5$ and $Ra = 10^5$). It is found that as the oscillation period increases, the heat has more time to interact with the flow field and as a result, the amplitude of oscillation for both Nu_m and θ_{max} increases. It must be pointed out that for values of τ_p above 10, increasing τ_p results in insignificant changes of Nu_m and θ_{max} oscillation.

In order to have a better understanding of the influence of the oscillation period on the cooling process using both the nanofluid and pure water, the variations of the highest and lowest values of θ_{max} with the oscillation period are plotted in Fig. 12. $(\theta_{max})_{max}$ has an initial increase for oscillation periods up to $\tau_p = 10$ and then remains unchanged. $(\theta_{max})_{min}$, however, decreases first and then remains unchanged for $\tau_p \ge 10$. This trend is observed for both pure water and the nanofluid. A reduction in the highest and lowest values of θ_{max} is also evident after the addition of nanoparticles into the pure water; this reduction, however, is negligible for $(\theta_{max})_{min}$ at high oscillation period values.

8. Conclusions

Natural convection cooling of an oscillating heat source embedded on the left wall of an enclosure filled with nanofluids has been numerically studied. The effects of various pertinent parameters such Rayleigh number, solid volume fraction, heat source position, type of nanofluid and oscillation period on the cooling performance of the enclosure are examined. The results of the present numerical analysis lead to the following conclusions:

- The oscillating heat flux generated by the heat source causes fluctuating behaviours for the flow and temperature fields as well as the heat source thermal parameters such Nu_m and θ_{max}. The oscillations of such parameters follow the heat source oscillation with a similar response frequency but with a slight phase shift.
- Increasing Rayleigh number is associated with increasing the strength of buoyant flow circulation cells, enhancing the heat removal from the heat source and therefore, decreasing the heat source maximum temperature.
- The addition of nanoparticles into the pure water improves its thermal conductivity and enhances the heat removal from the heat source. At low Rayleigh numbers, where the conduction is the main heat transfer mechanism, this effect is more noticeable such that the addition of 20% Cu nanoparticles results in a 37% reduction of the heat source maximum temperature.
- The influence of the heat source position is a function of Rayleigh number. That is to say for the best cooling performance, the heat source should be positioned in the middle of the left wall for low Rayleigh numbers, however, for high Rayleigh numbers it should be located at the bottom of the left wall.
- The type of nanoparticles also influences the enhancement of heat source cooling process. For all values of Rayleigh number and solid volume fraction, Cu and TiO_2 are the most and the least effective nanoparticles, respectively, in the heat removal process.
- For both pure water and a nanofluid, as the oscillation period of heat generation increases, the amplitudes of Nu_m and θ_{max} oscillations increase. This increase is more noticeable for oscillation periods below 10 and becomes negligible for oscillation periods above 10.
- The authors believe that the findings of this research study will provide useful information for the electronic industry to help maintain electronic components with oscillating heat generation under effective and safe operational conditions.

References

[1] S. Ostrach, Natural convection in enclosures, J. Heat Transf. 110 (1988) 1175–1190.
[2] J.L. Lage, A. Bejan, The resonance of natural convection in an enclosure heated periodically from the side, Int. J. Heat Mass Transf. 36 (8) (1993) 2027–2038.
[3] H.S. Kwak, J.M. Hyun, Natural convection in an enclosure having a vertical sidewall with time-varying temperature, J. Fluid Mech. 329 (1996) 65–88.
[4] H.S. Kwak, K. Kuwahara, H. Jae Min, Resonant enhancement of natural convection heat transfer in a square enclosure, Int. J. Heat Mass Transf. 41 (18) (1998) 2837–2846.
[5] M. Kazmierczak, A. Muley, Steady and transient natural convection experiments in a horizontal porous layer: the effects of a thin top fluid layer and oscillating bottom wall temperature, Int. J. Heat Fluid Flow 15 (1) (1994) 30–41.
[6] M. Kazmierczak, Z. Chinoda, Buoyancy-driven flow in an enclosure with time periodic boundary conditions, Int. J. Heat Mass Transf. 35 (6) (1992) 1507–1518.
[7] Q. Xia, K.T. Yang, D. Mukutmoni, Effect of imposed wall temperature oscillations on the stability of natural convection in a square enclosure, Trans. ASME J. Heat Transf. 117 (1) (1995) 113–120.
[8] B.V. Antohe, J.L. Lage, Experimental investigation on pulsating horizontal heating of a water-filled enclosure, Trans. ASME J. Heat Transf. 118 (4) (1996) 889–896.
[9] S.U.S. Choi, Enhancing thermal conductivity of fluids with nanoparticles, ASME Fluids Eng. Div. 231 (1995) 99–105.
[10] K. Khanafer, K. Vafai, M. Lightstone, Buoyancy-driven heat transfer enhancement in a two-dimensional enclosure utilizing nanofluids, Int. J. Heat Mass Transf. 46 (19) (2003) 3639–3653.
[11] R.Y. Jou, S.C. Tzeng, Numerical research of nature convective heat transfer enhancement filled with nanofluids in rectangular enclosures, Int. Comm. Heat Mass Transf. 33 (6) (2006) 727–736.

[12] G. Polidori, S. Fohanno, C.T. Nguyen, A note on heat transfer modelling of Newtonian nanofluids in laminar free convection, Int. J. Therm. Sci. 46 (8) (2007) 739–744.
[13] A.G.A. Nnanna, Experimental model of temperature-driven nanofluid, J. Heat Transf. 129 6 (2007) 697–704.
[14] N. Putra, W. Roetzel, S.K. Das, Natural convection of nano-fluids, Heat Mass Transf. 39 (8–9) (2003) 775–784.
[15] D. Wen, Y. Ding, Formulation of nanofluids for natural convective heat transfer applications, Int. J. Heat Fluid Flow 26 (6) (2005) 855–864.
[16] A.K. Santra, S. Sen, N. Chakraborty, Study of heat transfer characteristics of copper-water nanofluid in a differentially heated square cavity with different viscosity models, J. Enhanced Heat Transf. 15 (4) (2008) 273–287.
[17] C.J. Ho, M.W. Chen, Z.W. Li, Numerical simulation of natural convection of nanofluid in a square enclosure: effects due to uncertainties of viscosity and thermal conductivity, Int. J. Heat Mass Transf. 51 (17–18) (2008) 4506–4516.
[18] H.F. Oztop, E. Abu-Nada, Numerical study of natural convection in partially heated rectangular enclosures filled with nanofluids, Int. J. Heat Fluid Flow 29 (5) (2008) 1326–1336.
[19] A. Akbarinia, A. Behzadmehr, Numerical study of laminar mixed convection of a nanofluid in horizontal curved tubes, Appl. Therm. Eng. 27 (2007) 1327–1337.
[20] S. Palm, G. Roy, C.T. Nguyen, Heat transfer enhancement with the use of nanofluids in a radial flow cooling system considering temperature dependent properties, Appl. Therm. Eng. 26 (2006) 2209–2218.
[21] B. Ghasemi, Mixed convection in a rectangular cavity with a pulsating heated electronic component, Numer. Heat Transf. A Appl. 47 (5) (2005) 505–521.
[22] S.V. Patankar, Numerical Heat Transfer and Fluid Flow, Hemisphere Publishing Corporation, Taylor and Francis Group, New York, 1980, pp. 113–137.
[23] H.C. Brinkman, The viscosity of concentrated suspensions and solution, J. Chem. Phys. 20 (1952) 571–581.
[24] J. Maxwell, A Treatise on Electricity and Magnetism, second ed. Oxford University Press, Cambridge, UK, 1904, pp. 435–441.
[25] G. De Vahl Davis, Natural convection of air in a square cavity, a bench mark numerical solution, Int. J. Numer. Meth. Fluid. 3 (1983) 249–264.
[26] N.C. Markatos, K.A. Pericleous, Laminar and turbulent natural convection in an enclosed cavity, Int. J. Heat Mass Transf. 27 (5) (1984) 755–772.
[27] G.V. Hadjisophocleous, A.C.M. Sousa, J.E.S. Venart, Predicting the transient natural convection in enclosures of arbitrary geometry using a nonorthogonal numerical model, Numer. Heat Transf. A 13 (1998) 373–392.
[28] R.K. Tiwari, M.K. Das, Heat Transfer augmentation in a two-sided lid-driven differentially heated square cavity utilizing nanofluids, Int. J. Heat Mass Transf. 50 (2007) 2002–2018.